# Dynamic scattering function for high-temperature liquid lead

O. Söderström, U. Dahlborg, and M. Davidovič*
*Department of Reactor Physics, The Royal Institute of Technology, S-10044 Stockholm, Sweden*
(Received 17 May 1982)

Liquid lead at 1173 K has been studied by the thermal neutron scattering technique. The symmetrized scattering function is obtained at constant momentum transfers from 1.8 to 7.1 $\text{Å}^{-1}$. The highest observable energy transfer is 8 meV for the lowest momentum transfers and 28 meV for the highest. The measurement is corrected for experimental effects and special care has been given to the multiple-scattering corrections and subtraction of the container background. The first two even moments of the scattering function are determined and compared to an independent diffraction measurement and theoretical values, respectively. The full width at half maximum of the symmetrized scattering function is determined up to the ideal gas limit and compared with the corresponding quantity obtained at a lower temperature.

## I. INTRODUCTION

The neutron scattering technique is a powerful method for investigating the dynamical structure of condensed matter, since the neutron wavelength is of the same order of magnitude as the interatomic spacing, and the neutron energy is in the same range of energy as the atomic motions. The liquid state has extensively been studied with this experimental method, and the obtained results have stimulated theoretical efforts to explain the specific liquid behavior.[1,2]

Collective properties in liquids can advantageously be studied if the neutron cross section is fully coherent. With a low melting point the temperature dependence of various quantities can be observed. Lead has a coherent cross section[3] $\sigma_B^c = 11.37$ b and the melting point is low (600 K). Therefore it has been the subject of earlier measurements.[4,5] In Ref. 5 a complete list of references on neutron measurements on liquid lead is given. One recent measurement with cold neutrons at two temperatures shall be added.[6] The temperature dependence of cooperative modes has also been studied earlier with cold neutrons.[7]

By the use of the conventional thermal neutron scattering technique it is possible to cover large energy transfers ($E$ values) for wave-vector transfers ($Q$ values) from the position of the first peak in the structure factor ($Q_0$) and upwards. The temperature dependence of the scattering function informs about the influence of the kinetic energy on the liquid structure. For very large $Q$ values the dynamics of free atoms is seen, while for lower values the effect of various collision processes is observed.

In Sec. II some theoretical background is given. The experiment is fully discussed in Sec. III, and in Sec. IV the data reduction procedures are explained. The results are presented in Sec. V and discussed in Sec. VI. Finally, some conclusions are given in Sec. VII.

## II. THEORY

In a neutron experiment, with the time-of-flight method, the double differential cross section is measured for different scattering angles and flight times. By interpolation procedures this quantity can be obtained for constant $Q$ values and different energy transfers. Textbooks in theory of thermal neutron scattering[8,9] give the relation

$$\frac{d^2\sigma}{d\Omega dE} = \frac{\sigma_B^c}{4\pi}\left[\frac{E_0 - E}{E_0}\right]^{1/2} S(Q,E) , \tag{1}$$

where $\Omega$ is the solid angle, $\sigma_B^c$ the bound-atom cross section, $E_0$ the incoming neutron energy, $E$ the energy transferred to the scattering system, and $S(Q,E)$ the dynamic scattering function.

The symmetrized scattering function is defined by

$$\tilde{S}(Q,E) = e^{-E/2k_BT} S(Q,E) , \tag{2}$$

where $k_BT$ is the temperature in energy units. The experimental symmetrized scattering function can be compared to the scattering function obtained from classical theories of liquids.[10]

The zeroth moment of the coherent scattering function is equal to the structure factor, which means that an experimentally obtained scattering function can be compared to an independently measured quantity. The first and second moments shall

 

fulfil theoretically exact values. The quantity $E^2S(Q,E)$ represents the spectral function of the current-current correlations and has its main interest when determining the second moment.

Some models for the scattering function need the frequency moments $\langle\omega^n\rangle$ as input parameters. The fourth moment in $\omega_I^2=\langle\omega^4\rangle/\langle\omega^2\rangle$ is approximately given by

$$\omega_I^2=3\langle\omega^2\rangle+\omega_E^2\left[1-\frac{3\sin x}{x}-\frac{6\cos x}{x^2}+\frac{6\sin x}{x^3}\right], \tag{3}$$

where $x=QR_0$, and $R_0$ is approximately the distance between the nearest neighbors. The quantity $\omega_E^2$ is the weight of a delta function placed at $R_0$, and $\omega_E$ is of the same order of magnitude as the maximum phonon frequency in the solid.[1]

## III. EXPERIMENTAL DETAILS

The experiment was performed in the hybrid time-of-flight spectrometer for thermal neutrons at the reactor R2 in Studsvik. The instrument is fully described elsewhere.[11]

When performing a high-temperature measurement in a liquid metal, the requirements on the container material are extremely high. The container must, of course, be able to stand the temperature but also to be uneffected by long-time exposition to the corrosive metal. In this particular experiment silica was chosen as container material. Nine tubes were arranged vertically in a transmission geometry making an angle of 45° to the incident beam. The outer diameter of a single tube was 5 mm and the inner one was 3.8 mm. The distance between the tube centers was 5.4 mm. The container was heated electrically by a resistance wire made of KANTHAL wound around each tube. In order to decrease the heat radiation losses and temperature gradients, the whole container was wrapped with the silica cloth REFRASIL.

The incoming neutron energy was 47.7 meV corresponding to a neutron wavelength of 1.31 Å. The detectors were placed at scattering angles from 18.0° to 104.8°, and the flight path was 1.67 m. This detector arrangement implied that the accessible $Q$ range was from 1.5 to 7.6 $\text{Å}^{-1}$ for elastically scattered neutrons.

The kinematic region covered by the experiment was limited by the difficulty of separating the sample intensity from the relatively high container background at large energy transfers. Around $Q_0$ (2.2 $\text{Å}^{-1}$ for liquid lead) the scattering function is narrow, and the largest observable energy transfer was 8 meV. For higher $Q$ values the largest energy transfer was 28 meV.

The energy resolution for elastically scattered neutrons was obtained from a vanadium measurement. It varied from 1.7 to 3.5 meV over the observed $Q$ region. The $Q$ resolution was nearly constant 0.1 $\text{Å}^{-1}$.

## IV. DATA REDUCTION

In general, the background intensity is subtracted from the sample measurement directly in the raw data form. The multiple scattering in the background itself is then also subtracted. The multiple-scattering contribution is calculated by simulating the whole experiment including a surrounding container, which means that the multiple scattering in the container is included. This quantity, however, has already been removed from the data sets when the background was subtracted. Consequently, with this method of data correction, the multiple scattering in the container is corrected for twice. To overcome this inadequate procedure, the background and sample measurements shall be treated as two independent measurements, and the background is to be removed at the end of the data reduction process.

### A. Experimental effects

Both the sample and the background data sets were corrected for well-known experimental effects. Also, the influence of the detector wall on the detector efficiency was considered.[12] The system of computer programs is described elsewhere.[13] The results from this procedure were scattering functions normalized to the vanadium cross section and given as a function of the scattering angle and energy transfer.

### B. Multiple scattering

The multiple-scattering contribution was calculated by simulating the experiment by the Monte Carlo Method.[14] The program was modified so that the multiple scattering in the container could be calculated separately.

The container was made of vitreous silica, the structure of which was liquidlike and, thus, a structure factor could be defined. Following some initial ideas of Pelizzari and Sköld (private communication), the program was changed for this type of scattering. The modification was made in the incoherent scattering mode with the structure factor included. The normalization of the fluxes in the

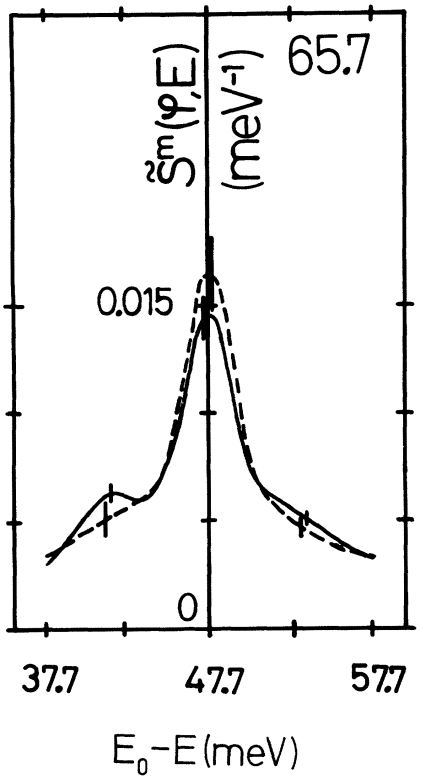


FIG. 1. Symmetrized scattering function for the multiple-scattering contribution at a constant angle (in degrees) versus energy of the scattered neutron. The full line is obtained with 15 000 neutrons in the Monte Carlo simulation and the dashed line with 3500. The statistical error bars are also shown.

scattering geometry was also slightly modified. In a calculation a scattering function is needed. However, in the $Q$ and $E$ regions covered in this experiment, no experimental results are available (Leadbetter and Wright, private communication). Therefore the inelastic scattering function of silica was approximated by a Gaussian function, the width of which was $Q$ dependent. The width was determined by least-squares fits to the measured intensity distributions. The total scattering function for silica $\tilde{S}^b(Q,E)$ was written as

$$\tilde{S}^b(Q,E)=e^{-2W}S(Q)\delta(E) + (1-e^{-2W})S(Q)f_Q(E)\,, \quad (4)$$

where $2W$ is the Debye-Waller factor, $S(Q)$ the structure factor, and $f_Q(E)$ the normalized Gaussian function mentioned above. The structure factor and the Debye-Waller factor of silica at room temperature was measured earlier.[15]

In order to determine whether the structure of the silica tubes was strictly amorphous and isotropic, an independent diffraction experiment was performed with different orientations of the tubes. The measured intensities gave no indication of anisotropy. It was also shown that the structure factor of Lorch[15] could be used as a zeroth-order approximation.

Using the scattering function given in Eq. (4), a multiple-scattering calculation was made with 2500 neutrons. The number density was slightly increased in order to include influences from the surrounding silica cloth. For one single scattering angle (65.7°) an extended calculation was made with 15 000 neutrons. The result showed very weak inelastic peaks, which were nearly invisible with 2500 neutrons.

In order to describe the scattering function at 1173 K for lead, the model of Ailawadi, Rahman, and Zwanzig[16] was used. The input parameters were the structure factor[17] and the fourth moment from Eq. (3). The parameter $R_0$ was chosen to the position of the first maximum of the pair distribution function[17] and $\omega_E$ to the maximum frequency of the "dispersion relation" at 623 K[18] with account taken to the temperature difference. The values used were $R_0=3.5$ Å and $\omega_E=10^{13}s^{-1}$. The calculation was made with 3500 neutrons. Here also an extended calculation was made with 15 000 neutrons for the same scattering angle as above (i.e., 65.7°). The results are presented in Fig. 1. It is seen that inelastic peaks appear in the extended calculation although the statistical error bars decreased very slowly with the number of neutrons used.

The multiple scattering in the vanadium slab used for the normalization run was also calculated[14,19] and found to be about 10%. The calculated multiple-scattering contributions described above were subtracted from the two measurements, and the corrections for self-shielding were finally applied.

### C. Subtraction of background

The background measurement was subtracted from the sample measurement, and the screening of the background by the sample was taken into account. However, after this procedure and subtraction of the computed multiple scattering there remained some inelastic peaks in the data. They were less clearly seen for the one angle (65.7°) for which extended multiple-scattering calculations were carried out (see Sec. IV B). The peaks did not disappear completely for this angle, because even with 15 000 neutrons the statistical error bars in the simulated results were not negligible (cf. Fig. 2). Since the computation time for such calculations was very long, they could be performed for this one angle only. It is most probable, however, that the same effect would be observed with extended calcu-

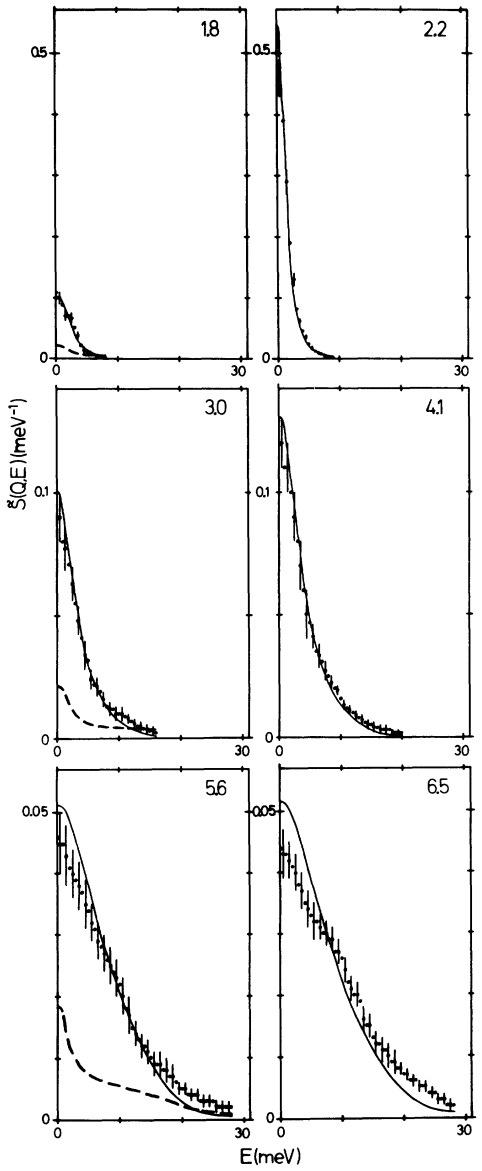


FIG. 2. Symmetrized scattering function for different energies and constant $Q$ values (in $\text{Å}^{-1}$). The dots with the error bars are from this experiment. The full line is the model in Ref. 16 folded with the resolution function. The dashed line is the multiple-scattering contribution from the sample with the container.

lations for all angles. Therefore the remaining inelastic peaks were removed by hand.

### D. Conversion to constant $Q$

The data sets of the sample, corrected for multiple scattering and background effects, were converted to constant $Q$ values.[13] The first two even moments were calculated. The same procedure was applied to the background.

The resolution function is included in the final results because there is no reliable method of deconvolution even if some recent attempts have been made.[20–22] A promising method is not directly applicable to this case since it needs some modifications,[23] which are under way.

## V. RESULTS

The symmetrized scattering function as a function of energy transfers for some $Q$ values is shown in Fig. 2. The same quantity is shown in Fig. 3 but now as a function of $Q$ for different energy transfers. The spectral function of the longitudinal current-current correlations is presented in Fig. 4. In all figures the model of Ailawadi, Rahman, and Zwanzig,[16] folded with a Gaussian resolution function of constant energy width, is included. The structure factor used in the model is the zeroth moment of the obtained scattering function. The parameters in the fourth moment are the same as those discussed in Sec. IV B above. It is to be emphasized that the model is shown in the figures solely because it was used in the multiple-scattering calculation. No physical significance will be given to the model, and it will not be discussed any further.

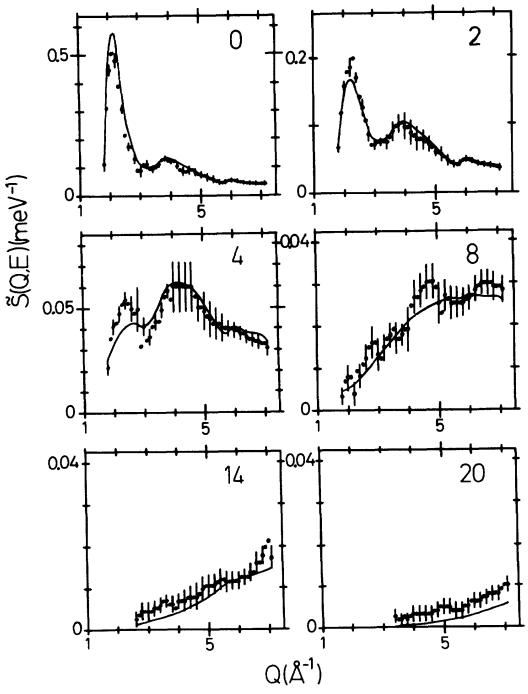


FIG. 3. Symmetrized scattering function for different $Q$ values and constant energy transfers (in meV). The notations are the same as in Fig. 2.

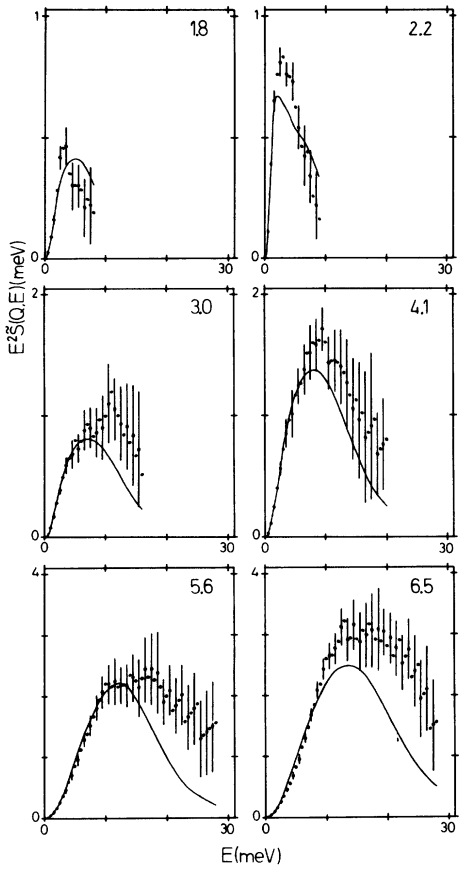


FIG. 4. Spectral function of current-current correlations for different energies and constant $Q$ values (in $Å^{-1}$). The notations are the same as in Fig. 2.

In Fig. 5 the zeroth moment of the scattering function is compared to an independent diffraction measurement.[17] The second moment is compared to the exact theoretical values in Fig. 6. In Fig. 7 the full width at half maximum (FWHM) of the symmetrized scattering function at two temperatures, 1173 and 623 K, is given. The experimental resolution function was removed by assuming a Gaussian resolution function and a Lorentzian shaped scattering function. For comparison the FWHM of the incoherent scattering function, describing a diffusive motion, is included. The full curve close to the measurement at 623 K refers to a self-diffusion constant measured earlier.[24] The self-diffusion constant at 1173 K was calculated with a hard-sphere model with back scattering effects included.[25,26] The packing fraction was obtained from Ref. 17. Also, this full curve is included in Fig. 7. The dashed line is the width function of an ideal gas of Pb atoms at 1173 K.

As a by-product of this experiment, the scattering function for silica at 1173 K was obtained. The zeroth moment is shown in Fig. 8 together with an independently measured structure factor.[15] The second moment is about 40% higher than the expected theoretical values.

## VI. DISCUSSION

As mentioned above and also presented in Fig. 1, the extended multiple-scattering calculation for the sample showed peaks in the inelastic part of the calculated spectra. These peaks are originating from scattering processes involving an inelastic event in lead and an elastic event in silica, which has a pronounced structure. The same effect was also observed in bare silica but much less clearly since the inelastic scattering as a whole was small. During the Monte Carlo simulation these particular scattering processes, however, occurred rather seldom implying a large statistical error in the result. In Sec. IV C it was discussed why the extended multiple-scattering calculations could be performed only in a limited region. The inelastic peaks were seen for all scattering angles above 40° both in the intensity from the sample measurement and, though less clearly, in the background. A general observation is that the peaks were more pronounced in the experiments than in the simulations. The explanation is

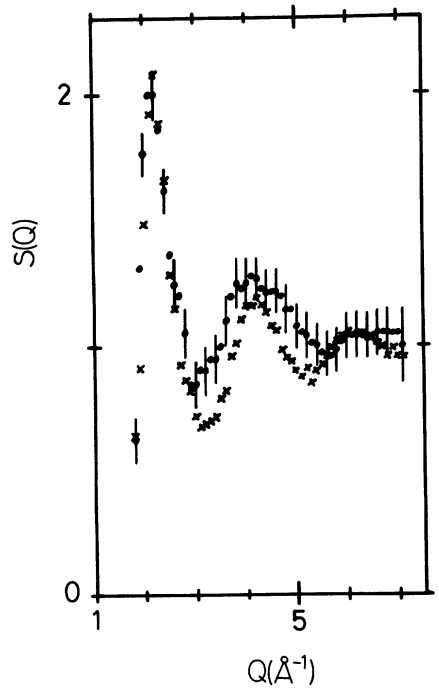


FIG. 5. Structure factor of liquid lead. The dots with error bars are from the experimental scattering function integrated over $E$ for every $Q$ value, and the crosses are from an independent diffraction measurement in Ref. 17.

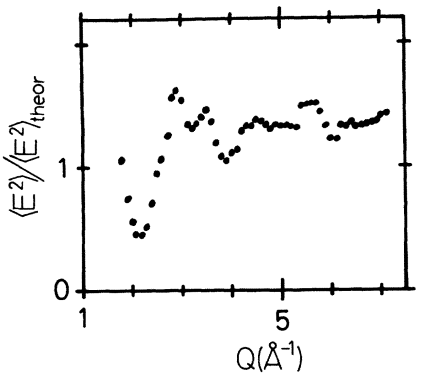


FIG. 6. Second moment of the experimental scattering function compared to the exact theoretical value with the zeroth moment from Fig. 5.

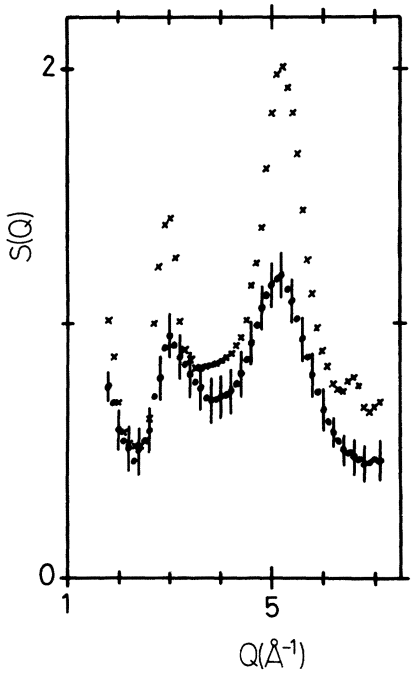


FIG. 8. Stucture factor for silica at 1173 K. The dots with error bars refer to this measurement. The crosses are from an independent neutron-diffraction measurement in Ref. 15 measured at room temperature.

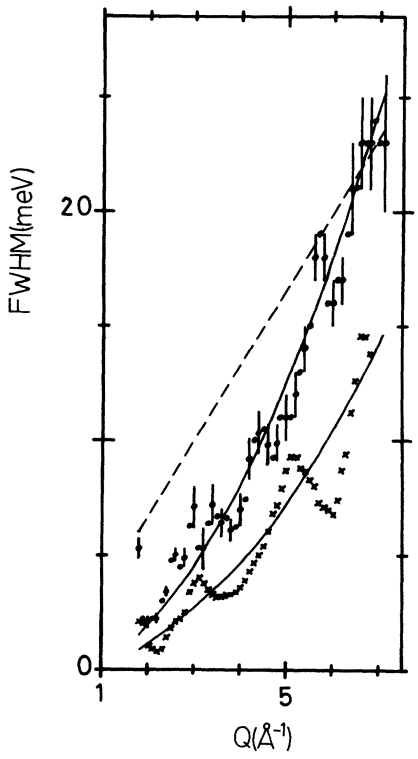


FIG. 7. FWHM of the symmetrized scattering function. The dots with error bars are from the obtained experimental natural widths at 1173 K. The crosses are the same quantity at 623 K. The correction for the resolution is treated in the text. The two parabolas correspond to the diffusion constants at the two temperatures, respectively. The dashed line represents an ideal gas model at 1173 K.

that in the former cases the statistical accuracies are considerably better. In this context it should be noticed that the scattering processes discussed here always are present and that the effect is by no means unique for this particular experiment. Furthermore, for a tube container in general, there is a high probability for an elastic scattering event in the wall combined with an inelastic process in the sample, especially when the ratio of the inner diamater to the neutron mean free path is small. However, usually the container scattering is low and a tube geometry can be avoided. The inelastic peaks are then hidden in statistical uncertainties. In this experiment it was necessary to use tubes, whose scattering power was of the same order of magnitude as that of the sample.

The models used in the multiple-scattering calculations are, at least for silica, to be regarded as zeroth-order approximations. However, it has been shown that considerably different structure factors have influence only on the simulated results for very small $Q$ values.[27] The calculated multiple-scattering contributions were subtracted from the experimental values and were therefore not very sensitive to the model used.[1] Furthermore, the multiple scattering as a whole was fairly small as can be seen in Fig. 2. Regarding these aspects, no iterative calculations were performed with the obtained scattering func-

tions as input kernel. The accuracy of the multiple-scattering corrections is completely determined by the obtained statistical errors, which in turn depend on the number of neutrons used.

In the observed $Q$ region no structure is observed in the scattering function when displayed for constant $Q$ values. For constant energy transfers the structure is more apparent (Figs. 2 and 3). This was also observed at 623 K.[5] The spectral function of the current-current correlations is shown here only to demonstrate the difficulty to determine the second moment because of limited observable $E$ range and large error bars (Fig. 4). The irregularity of both the experimental values and the model around $Q_0$ is a resolution effect.[5] The zeroth moment differs from the structure factor, especially around 2.5 and 5 $\text{Å}^{-1}$ (Fig. 5). For these $Q$ values the silica structure factor has peaks, and consequently, the background is more difficult to subtract (Fig. 8). The depression of the second moment around $Q_0$ is due to truncations of the spectra (Fig. 6). At larger $Q$ values the second moment is, on the average, about 30% too high, which with regard to the difficulties involved in this type of experiment is satisfactory.

The *incoherent* scattering function describes the self-motion of atoms. For simple diffusion it is, for small $Q$ values, given by a Lorentzian with a width function quadratic in $Q$, determined by the self-diffusion constant. For an ideal gas the scattering function is a Gaussian with a width function linear in $Q$. The FWHM curves for the *coherent* scatterers argon and lead near the melting point both oscillate around the diffusion parabola even for large $Q$ values, but they are still far away from the ideal gas behavior.[5,28] For liquid rubidium (also a coherent scatterer) the FWHM curve is quite different as the oscillations do not occur around the diffusion parabola. The experimental values nearly reach the ideal gas line for large $Q$ values.[29]

To investigate if the FWHM curve for lead at 1173 K follows a parabola, it was plotted against $Q^2$. It was found that a least-squares fit could be done with a straight line through the origin. The obtained value of the slope was very near the calculated value of the self-diffusion constant at this temperature mentioned in Sec. V above. This value is about a factor of 2 less than the results from diffusion experiments for slightly lower temperatures.[24] For large $Q$ values the FWHM curve reaches the curve that is determined by the ideal gas model.

The zeroth moment of the scattering function for silica differs from the values obtained from a diffraction measurement.[15] The discrepancies are large around the peaks at 3 and 5 $\text{Å}^{-1}$. A possible explanation is that the silica qualities are not the same in the two experiments. However, the diffraction experiment mentioned in Sec. IV B above, looking for orientational effects, indicated that the structure factor in our case is closer to the obtained zeroth moment. Both this diffraction experiment and the measurements by Lorch[15] were performed at room temperatures, while the zeroth moment was determined at 1173 K.

## VII. CONCLUSIONS

In a liquid metal near the melting point the atoms are arranged in a fairly well-developed structure, because the potential energy is high. When the temperature increases, the kinetic energy grows large, and the structure is less pronounced. This smearing-out effect is mainly seen in the structure factors but also in the scattering functions presented for constant energy transfers.

Kinetic theories[30,31] have shown that the self-motion is important for the shape of the coherent scattering function at all experimentally accessible $Q$ values. Recently, the FWHM curves of the incoherent scattering functions for argon and rubidium have been calculated and compared with the ones assuming self-diffusion.[32] For argon the difference between the two curves was at most 20% and for rubidium 60%. This observation may explain why the FWHM of the coherent scattering function fluctuates around the self-diffusion parabola for argon, while for rubidium it deviates clearly. The measured FWHM for lead at 623 K is similar to that of argon,[28] which then indicates that the self-motion in lead is more diffusionlike than in rubidium. As discussed above this is even more pronounced when the temperature is increased, and the effect maintains up to the ideal gas limit.

Collective excitations have been observed in liquid lead close to the melting point. Criteria for their existance have been formulated,[33] and a temperature study at small $Q$ values would give important information on the possibility for a liquid metal to sustain these modes of motion. For instance, the role played by the structure factor would be made clear. However, such an experiment has extremely high requirements on its performance, among other things the choice of container material and available primary neutron flux.

## ACKNOWLEDGMENTS

The Swedish National Science Research Council has supported this experiment financially. Mr. L. E. Karlsson and Mr. M. Grönros are acknowledged for skilful technical assistance. One of the authors (M.D.) is much indebted to the staff of the Department of Reactor Physics for their hospitality during his stay in Stockholm.

*On leave of absence from The Boris Kidrič Institute of Nuclear Science, Vinča, Belgrade, Yugoslavia. Now returned.

[1]J. R. D. Copley and S. W. Lovesey, Rep. Prog. Phys. 38, 416 (1975).

[2]S. W. Lovesey and J. R. D. Copley, *Neutron Inelastic Scattering 1977* (International Atomic Energy Agency, Vienna, 1978), Vol. II, p. 3.

[3]L. Koester, *Springer Tracts in Modern Physics, Neutron Physics* (Springer, Berlin, 1977), Vol. 80, p. 1.

[4]O. Söderström. M. Davidovič. U. Dahlborg, and K. E. Larsson, Ref. 2, p. 67.

[5]O. Söderström, Phys. Rev. A 23, 785 (1981).

[6]I. Pădureanu, S. Râpeanu, G. H. Rotărescu, and C. Crăciun, Rev. Roum. Phys. 24, 805 (1979).

[7]G. D. Wignall and P. A. Egelstaff, J. Phys. C 1, 519 (1968).

[8]G. L. Squires, *Introduction to the Theory of Thermal Neutron Scattering* (Cambridge University Press, Cambridge, England, 1978).

[9]W. Marshall and S. W. Lovesey, *Theory of Thermal Neutron Scattering* (Oxford University Press, Oxford, England, 1971).

[10]P. Schofield, Phys. Rev. Lett. 4, 239 (1960).

[11]L. G. Olsson, U. Dahlborg, M. Grönros, L. E. Karlsson, K. E. Larsson, and T. Månsson, Nucl. Instrum. Methods 123, 99 (1975).

[12]M. Davidovič and U. Dahlborg, Nucl. Instrum. Methods 142, 601 (1977).

[13]O. Söderström, thesis, The Royal Institute of Technology, Stockholm, 1980 (unpublished).

[14]J. R. D. Copley, Comput. Phys. Commun. 7, 289 (1974); 20, 459 (1980).

[15]E. Lorch, J. Phys. C 3, 1314 (1970).

[16]N. K. Ailawadi, A. Rahman, and R. Zwanzig, Phys. Rev. A 4, 1616 (1971).

[17]U. Dahlborg, M. Davidovič, and K. E. Larsson, Phys. Chem. Liq. 6, 149 (1977).

[18]O. Söderström. J. R. D. Copley, J. -B. Suck, and B. Dorner, J. Phys. F 10, L151 (1980).

[19]J. R. D. Copley, Comput. Phys. Commun. 9, 54 (1975).

[20]I. Beniaminy and M. Deutsch, Comput. Phys. Commun. 21, 271 (1980).

[21]H. Fredrikze and P. Verkerk, Comput. Phys. Commun. 24, 5 (1981).

[22]I. Beniaminy and M. Deutsch, Comput. Phys. Commun. 24, 9 (1981).

[23]J. Philip, IEEE PAMI-1, 385 (1979).

[24]N. H. Nachtrieb, Adv. Phys. 16, 309 (1967).

[25]T. E. Faber, *An Introduction to the Theory of Liquid Metals* (Cambridge University Press, Cambridge, England, 1972).

[26]M. Shimoji, *Liquid Metals* (Academic, London, 1977).

[27]U. Dahlborg and L. G. Olsson, J. Phys. (Paris) 41, C8-214 (1980).

[28]K. Sköld, J. M. Rowe, G. Ostrowski, and P. D. Randolph, Phys. Rev. A 6, 1107 (1972).

[29]J. R. D. Copley and J. M. Rowe, Phys. Rev. A 9, 1656 (1974).

[30]L. Sjögren and A. Sjölander, Ann. Phys. (N.Y.) 110, 122 (1978); 110, 421 (1978).

[31]L. Sjögren, Ann. Phys. (N.Y.) 110, 156 (1978).

[32]G. Wahnström and L. Sjögren, J. Phys. C 15, 407 (1982).

[33]O. Söderström, J. R. D. Copley, J. -B. Suck, and B. Dorner, J. Phys. (Paris) 41, C8-230 (1980).